

Study of the Adsorption and Desorption of Zn(II) and Pb(II) on CaF₂ Nanoparticles

Barrak, Haythem*⁺

Centre National des Recherche en Sciences des Matériaux, Laboratoire de Valorisation des Matériaux Utiles (LVMU), Technopole Borj Cedria, BP 73 Soliman 8027, TUNISIA

Kriaa, Abdelkader

Ecole Nationale Supérieure d'Ingénieurs de Tunis, Laboratoire de Chimie Moléculaire Organique, 1008 Tunis, TUNISIA

Triki, Mohamed; M'nif, Adel; Hamzaoui, Ahmed Hichem

Centre National des Recherche en Sciences des Matériaux, Laboratoire de Valorisation des Matériaux Utiles (LVMU), Technopole Borj Cedria, BP 73 Soliman 8027, TUNISIA

ABSTRACT: This paper explores the adsorptive properties of CaF₂ nanoparticles for the removal of Pb(II) and Zn(II) from aqueous solutions and their selective recovery. CaF₂ nanoparticles were synthesized by a facile one-step reaction and characterized by N₂ physisorption at 77 K, XRD, and TEM. The adsorption of Zn(II) and Pb(II) fits well with Elovich and Langmuir isotherm models, respectively. Kinetic data are well described by the pseudo-second-order model. Our results show that Zn(II) and Pb(II) could be totally and selectively desorbed with HCl solution (0.01 M). The results of the competitive adsorption and desorption of Pb(II) and Zn(II) show that Zn(II) is desorbed before Pb(II) leading to a good separation. The desorption yield reaches 89% for Zn(II) and 95% for Pb(II), which opens the route to regenerate the adsorbent for other cycles.

KEYWORDS: Heavy metals; Adsorption; Desorption; Competition; CaF₂.

INTRODUCTION

Phosphogypsum (PG) is a solid waste from the wet processes of phosphoric acid production. Today, approximately 10 million tons of PG is produced annually by the Tunisian phosphate industry [1]. Such a huge amount of PG causes severe pollution to the surrounding environment due to some of its harmful components, such as soluble P₂O₅, heavy metals and organic substances [2]. As a consequence, it is urgent to dispose and utilize

this hazardous solid waste effectively. That's way, many researchers focused on its valorization in order to minimize storage costs and to reduce the negative public health and environmental impacts [3, 4]. For example, PG has been valorized in construction materials [5], as an agriculture fertilizer [6] and especially for its transformation into Na₂SO₄ and CaF₂ [7]. In this context, *Hajem et al.* [8] confirmed the formation of CaF₂ during

* To whom correspondence should be addressed.

+ E-mail: barrak.haythem@gmail.com

1021-9986/2020/5/191-201

11/\$/6.01

the neutralization of phosphogypsum. The obtained CaF_2 showed a very good ability to remove cadmium from wastewaters [9]. The remediation of heavy metals pollution from wastewaters is considered as one of the major environmental challenges [10, 11]. These pollutions affect the ecological environment or the living organisms [12]. Even though some analytical methods permit the detection of heavy metals [13], it is more interesting to proceed to their elimination by nanofiltration or reverse osmosis [14]. Adsorption appears as an efficient and cheap alternative for the elimination of heavy metals [15, 16]. Therefore, many adsorbents were studied such as activated carbon [17], biomaterials [18, 19], clays [20] and modified oxides [21-23]. In this study, the capacity of CaF_2 to remove heavy metals was studied. Different experimental conditions, involving pH, contact time, CaF_2 mass and temperature are investigated to understand and to optimize the adsorption of Zn(II) and Pb(II) from aqueous solution by CaF_2 . The adsorption behaviors of Zn(II) and Pb(II) on CaF_2 are explored by adsorption kinetics, isotherm models and thermodynamic parameters. The desorption study is conducted to investigate the possibility of recycling CaF_2 , and Zn(II) and Pb(II) ions recovery. The competitive adsorption and desorption of both metals is also investigated for their selective separation.

EXPERIMENTAL SECTION

Preparation of CaF_2

CaF_2 nanoparticles were prepared by a facile one-step reaction. Typically, 200 mL of NaF (0.25 M) was dropped slowly in 200 mL of CaCl_2 solution (0.25 M) under vigorous stirring for 2 h at 30°C. The mixture was then centrifuged for 15 min at 4000 rpm. After separation, the solid was washed with ultrapure water a several times and finally dried at 100 °C.

Characterization

The powder X-Ray Diffraction (XRD) pattern was measured on a Philips X-ray diffractometer Model PW 1730/10 (French) with Cu $K\alpha$ radiation ($\lambda=0.15418$ nm). The specific surface area was determined with Brunauer-Emmett-Teller (BET) method from N_2 adsorption-desorption isotherms at 77 K using a Quantachrom Autosorb-1 unit (USA). The degassing processes was accomplished under a vacuum at 10^{-3} mmHg for 4 h at 120°C. Transmission Electron Microscopy (TEM)

analysis was operated at 60-70 kV by a JEOL JEM-1200 microscope (USA). The sample was suspended and dispersed in ethanol by ultrasonic treatment. A drop of the fine suspension was placed on a copper grid into the microscope. The point of zero charge (pH_{PZC}) was determined by the solid addition method. CaF_2 (1 g) was introduced in two beakers containing 50 mL of KNO_3 (0.01 M). The initial pH (pH_i) was changed using NaOH (0.1 M) and HCl (0.1 M) solutions. After stirring for 24 h, the final pH (pH_f) was reached. $\Delta\text{pH} = (\text{pH}_f - \text{pH}_i)$ is plotted as a function of the initial pH, where pH_{PZC} is the intersection of the curve with the x-axis [24]. The speciation diagram of metals in aqueous medium is calculated using Visual Minteq software database (Sweden).

Adsorption experiments

Zn(II) and Pb(II) solutions (1000 ppm) were prepared using $\text{Zn}(\text{CH}_3\text{COO})_2 \cdot 2\text{H}_2\text{O}$ ($\geq 98\%$, Sigma-Aldrich,) and PbCl_2 (98%, Sigma-Aldrich), respectively. Batch experiments were conducted by mixing 1 g of CaF_2 with 50 mL of each solution at fixed temperature. The adsorption experiments were performed separately for both cations. The solid was separated from the mixture by centrifugation under 4000 rpm. Finally, the solutions were analyzed using Atomic Absorption Spectrometry (AAS) using a Vario 6 apparatus (Analytik Jena, Germany). The amount of metal ion adsorbed on CaF_2 is calculated according to:

$$q_e = \frac{(C_0 - C_e)V}{m} \quad (1)$$

Where C_0 and C_e are the initial and equilibrium concentrations (mg/L), respectively; V is the volume of the metal ion solution (L), and m is the mass of CaF_2 (g).

The adsorption capacity is calculated according to:

$$\%p = \frac{q_e}{q_m} * 100 \quad (2)$$

Where q_e and q_m are the amount adsorbed and the maximal quantity of ion (mg/g), respectively.

Desorption experiments

CaF_2 (1 g), after the adsorption, was introduced in 50 mL of water at $\text{pH}=4$ fixed with HCl (0.01 M). The conditions of desorption were established by studying the pH and the electrical conductivity of the solution (pH Meter/Conductometer Metrohm 914, Swaziland) at 298 K.

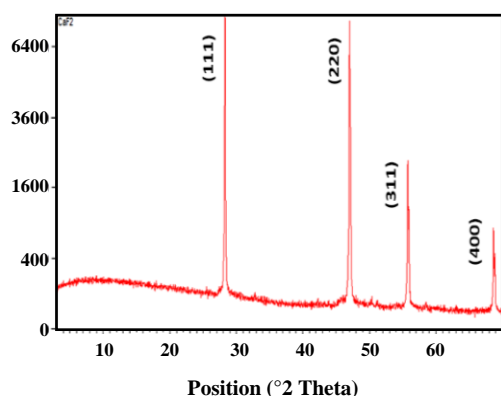


Fig. 1: XRD pattern of synthesized CaF₂.

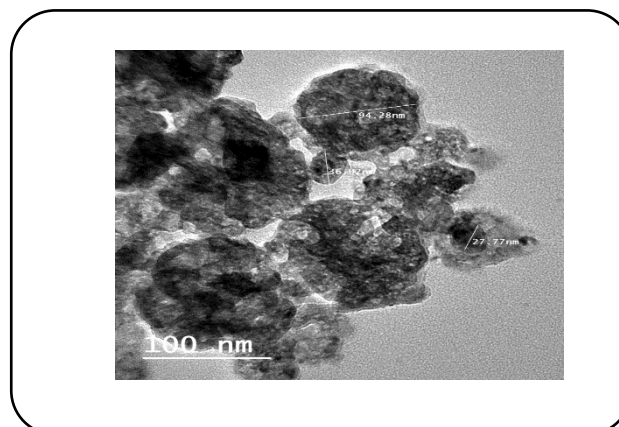


Fig. 2: TEM image of synthesized CaF₂ nanoparticles.

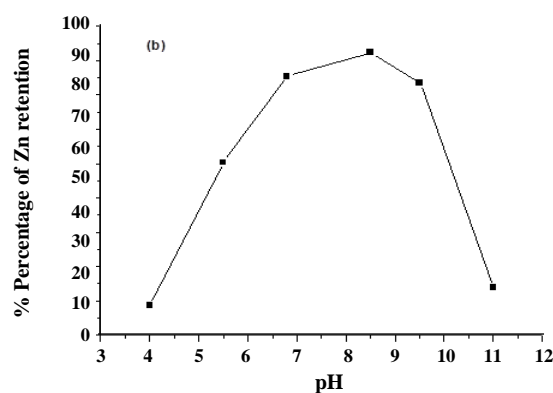
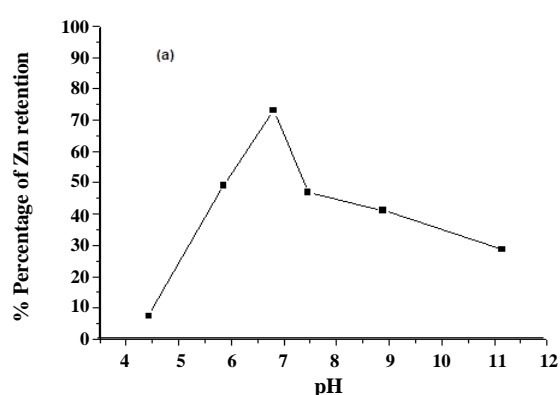


Fig. 3: Percentage of retention vs pH for (a) Zn(II) and (b) Pb(II) ([metal ion]=40 ppm; V_{sol} =50 mL; m_{CaF_2} =0.5 g).

The concentrations of desorbed Pb(II) and Zn(II) were determined by AAS. The percentage of desorption is given by:

$$\% \text{ desorption} = \frac{C_{des}}{C_{ads}} * 100 \quad (3)$$

where C_{ads} and C_{des} are the concentrations (mg/L) of adsorbed ion in optimal condition and desorbed ions, respectively.

RESULTS AND DISCUSSION

CaF₂ characterization

Fig. 1 shows the XRD pattern of synthesized CaF₂ indicating the presence of calcium fluoride (PDF-ICDD 00-035-0816). In fact, the diffraction peaks at $2\theta = 28.3, 47, 55.8$ and 68.7° correspond respectively to (111), (220), (311) and (400) reflections of cubic structure [25]. The BET surface area is equal to $42 \text{ (m}^2/\text{g)}$. The surface area is not very large compared to other specific surfaces area of adsorbents such as activated carbon [26]. These results are consistent with those found by Giudici *et al.* [27].

TEM image presented in Fig. 2 shows that the range of particle size of CaF₂ is between 25 and 100 nm.

Adsorption study

Effect of pH

The effect of pH on metals sorption is studied in the range of 4.0-11.0 since CaF₂ is not stable at pH lower than 3 showing a high solubility in HCl [28]. Fig. 3 shows the effect of pH on the retention percentage of Zn(II) and Pb(II) on CaF₂. The results show that maximum of retention of Zn(II) (73%) and Pb(II) (94%) are reached at pH of 6.8 and 8.6, respectively. The pH_{PZC} of CaF₂ is found to be 6 (Fig. 4). Therefore, a $pH > pH_{PZC}$ is required to facilitate the adsorption of these cations due the negative surface charges of CaF₂. At $pH = 6.8$, Zn(II) exists as Zn^{2+} unlike at $pH = 8.6$ Pb(II) is in the Pb^{2+} , $Pb(OH)^+$, $Pb_3(OH)_4^{2+}$ and $Pb(OH)_2$ forms as shown in Fig. S1 and Fig. S2 (Supplementary information). The adsorption of

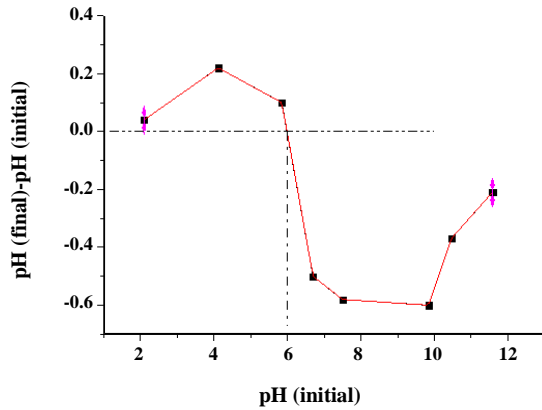


Fig. 4: Determination of the pH_{PZC} of synthesized CaF_2 ($m_{CaF_2}=1$ g; $V_{sol}=50$ mL; $T=298$ K).

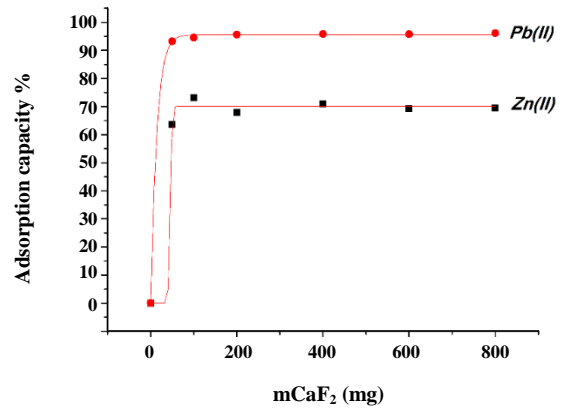


Fig. 5: Adsorption capacity of CaF_2 vs mass of CaF_2 ([metal ion]=40 ppm; $V_{sol}=50$ mL; $t=30$ min; $T=298$ K; $pH=6.8$ and 8.6 for Zn(II) and Pb(II)).

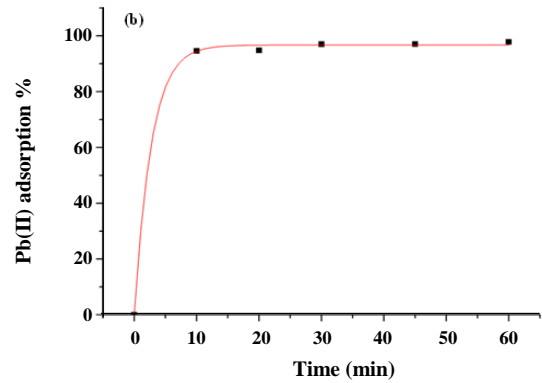
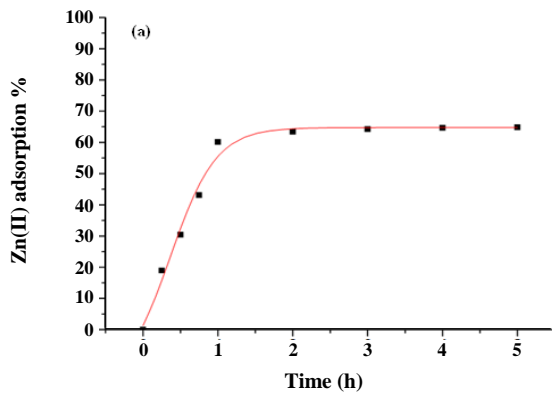


Fig. 6: Adsorption capacity of CaF_2 vs time for (a) Zn(II) and (b) Pb(II) ([metal ion]=40 ppm; $V_{sol}=50$ mL; $pH=6.8$ and 8.6 for Zn(II) and Pb(II); $m_{CaF_2}=250$ and 100 mg for Zn(II) and Pb(II)).

Zn(II) is limited to $pH < 7$ because $Zn(OH)_2$ precipitates from this value. On the other hand, $pH=9$ is the upper value for the adsorption of Pb(II) because it was found that $Pb(OH)_2$ is formed with significant amount.

Effect of CaF_2 mass

Fig. 5 shows the effect of CaF_2 mass on its adsorption capacity for Zn(II) and Pb(II). The result shows that a maximum of retention for Zn(II) and Pb(II) is reached at 30 min corresponding to 28.4 mg/g and 38.8 mg/g, respectively. Therefore, two optimal CaF_2 masses of 100 mg and 250 mg are chosen for the adsorption of Pb(II) and Zn(II), respectively.

Effect of contact time

The effect of contact time on the adsorption of Zn(II) and Pb(II) on CaF_2 is studied and the results are shown in Fig. 6.

It can be noticed that the adsorption of Pb(II) is faster than Zn(II). In fact, the adsorption of Pb(II) needs 10 min to reach 97%; however, the adsorption of Zn(II) needs 120 min to reach 65%.

Adsorption kinetics

The pseudo-first order and pseudo-second order models are used in this work, where their equations are expressed respectively by:

$$\ln(q_e - q_t) = \ln q_e - k_1 t \quad (4)$$

$$\frac{t}{q_t} = \frac{1}{k_2 q_e^2} + \frac{1}{q_e} t \quad (5)$$

Where q_e and q_t are the adsorption capacities (mg/g) at equilibrium and time t (min), respectively. k_1 is the pseudo-first order rate constant (min^{-1}) and k_2 is the pseudo-second order model rate constant ($\text{g}/(\text{mg min})$).

Table 1: Kinetic parameters for the adsorption of Zn(II) and Pb(II) on CaF₂.

Kinetic models	Parameters	Pb(II)	Zn(II)
Pseudo-first order	k_1 (min ⁻¹)	0.807	0.025
	R^2	0.741	0.944
Pseudo-second order	k_2 (g/(mgmin))	0.169	0.021
	R^2	0.999	0.995

The kinetic parameters obtained from the two models for the adsorption of Zn(II) and Pb(II) on CaF₂ are shown in Table 1. The results indicate that the pseudo-second order model fits well with the experimental data. In fact, the correlation coefficients (R^2) obtained with this model are 0.995 and 0.999 for the adsorption of Zn(II) and Pb(II), respectively (Fig. S3, supplementary information). This means that the overall rate of Zn(II) and Pb(II) adsorption process seems to be controlled by the chemical process through exchanging of electrons between adsorbent and adsorbate, the time of interaction and the concentrations of heavy metals [29].

Adsorption isotherms

To evaluate successfully the interaction adsorbate/adsorbent, four typical isotherm models (Langmuir, Elovich, Temkin and Dubinin-Radushkevich) are used describing the equilibrium. For Langmuir isotherm [30], the non-linear form is given by:

$$\frac{1}{q_e} = \frac{1}{q_m} + \frac{1}{q_m K_L C_e} \quad (6)$$

Where q_e and C_e are the adsorption capacity (mg/g) and the concentration (mg/L) at equilibrium, respectively; q_m and K_L represent the maximum adsorption capacity of adsorbents (mg/g) and the Langmuir adsorption constant (L/mg), respectively.

The Elovich isotherm model is presented at equilibrium by:

$$\log \left(\frac{q_e}{C_e} \right) = \log (K_E \times q_m) + \frac{q_e}{q_m} \quad (7)$$

where q_m is the maximum adsorption capacity (mg/g); q_e and C_e are the adsorption capacity (mg/g) and the concentration (mg/L) at equilibrium, respectively; K_E is the equilibrium constant of Elovich isotherm model.

Temkin proposed a model, which assumes that the heat of adsorption varies linearly with the amount adsorbed [31]. The linear form of Temkin isotherm is indicated by:

$$q_e = B \ln K_T + B \ln C_e \quad (8)$$

$$B = \frac{R T}{b} \quad (9)$$

Where R is the gas constant (8.341 (J/molK)), T is the absolute temperature (K), K_T is the equilibrium binding constant corresponding to the maximum binding energy (L/g), b is the Temkin isotherm constant and B represents isotherm constant related to the heat of adsorption (J/mol).

The Dubinin and Radushkevich (D-R) isotherm model [32] is presented by:

$$\ln q_e = \ln q_o - K_D \epsilon^2 \quad (10)$$

$$(\text{Polanyi potential}) = R T \ln \left(1 + \frac{1}{C_e} \right) \quad (11)$$

Where q_o is the D-R constant, the constant K_D gives the mean free energy per molecule (E) of the adsorbate when it is transferred to the surface of solid from infinity in the solution.

E (J/mol) is used to estimate the type of adsorption process (chemical or physical adsorption) and calculated from:

$$E = \frac{1}{\sqrt{2 \cdot K_D}} \quad (12)$$

If $E < 8$ (kJ/mol), physisorption dominates; if $8 < E < 16$ (kJ/mol), ion exchange dominates and if $E > 16$ (kJ/mol), the intra-particle diffusion dominates [33].

Table 2 regroups the isotherm parameters calculated from the Langmuir, Temkin, Elovich and D-R models.

For the adsorption of Pb(II), the result shows that the experimental data are well described with Langmuir isotherm model, which presents a correlation coefficient (R^2) of 1 (Fig. S4a, Supplementary information). Moreover, the Langmuir model leads to a calculated adsorbed quantity of 9.23 mg/g, which is the more accurate to the maximum quantity adsorbed at equilibrium

Table 2: Isotherms parameters for the adsorption of Zn(II) and Pb(II) on CaF₂.

Isotherm models	Parameters	Pb(II)	Zn(II)
Langmuir	q _m (mg/g)	9.23	2.22
	K _L (L/mg)	36.1	-0.122
	R ²	1	0.996
Elovich	q _m (mg/g)	0.35	1.82
	K _E (L/mg)	8.2 10 ⁻¹¹	0.12
	R ²	0.990	0.997
D-R	q _m (mg·mmol/g)	0.041	0.27
	K _D (mol ² /kJ ²)	-5.5 10 ⁻¹⁰	-5.7 10 ⁻⁸
	E (kJ/mol)	30	2.95
	R ²	0.990	0.988
Temkin	K _T (L/mol)	6.5 10 ⁻¹²	1.9 10 ⁻²
	ΔQ (kJ/mol)	-62.04	-1.14
	R ²	0.989	0.995

(q_m(exp)=18.40 mg/g) compared to other models. However, for the adsorption of Zn(II), the experimental data do not fit with the Langmuir isotherm model because the Langmuir adsorption constant has a negative value (K_L < 0) even if the R² is 0.996 and q_m(exp) is 5.60 mg/g (close to the calculated adsorbed quantity of 2.22 mg/g). However, the Elovich isotherm model leads to a correlation coefficient (R²) of 0.997 (Fig. S4b, Supplementary information) and a calculated adsorbed quantity of 1.82 mg/g. Taking into account these values, it can be concluded that the Elovich isotherm model describes well the adsorption of Zn(II).

Thermodynamic study

The thermodynamic behavior is studied *via* different parameters providing information on inherent energetic changes, which are associated to the adsorption [34]. These parameters are changes in: Gibbs free energy (ΔG°), standard entropy (ΔS°) and standard enthalpy (ΔH°), which could be calculated according to:

$$\Delta G^\circ = -RT \ln K^\circ \quad (13)$$

$$\ln K^\circ = \frac{\Delta S^\circ}{R} - \frac{\Delta H^\circ}{RT} \quad (14)$$

Where K° is equilibrium constant, T is absolute temperature (K), R is gas constant (R=8.314 J/(Kmol)).

Fig. 7 shows the effect of temperature on the adsorption of Zn(II) and Pb(II) on CaF₂. The standard entropy (ΔS°) and the standard enthalpy (ΔH°) changes are obtained

from the linear plot of lnK° versus 1/T. The thermodynamic parameters calculated from the adsorption isotherms at different temperatures are listed in Table 3. The positive values of ΔH° confirm the endothermic nature of adsorption, while the positive values of ΔS° reflect an increase in randomness at the solid/solution interface. The negative values of ΔG° indicate that the adsorption process is spontaneous. Moreover, the values of ΔG° decrease when temperature increases showing that the adsorption of Zn(II) and Pb(II) on CaF₂ is facilitated at high temperature.

Desorption study

The desorption experiments were carried out to explore the possibility of recycling of CaF₂. Therefore, the desorption of Zn(II) and Pb(II) was studied by following the evolution of pH and electrical conductivity in the course of time. The equations (15) and (16) presented the conductance and conductivity, respectively:

$$\sigma = \sum (\lambda_i C_i) \quad (15)$$

$$G = K \sum \lambda_i C_i Z_i \quad (16)$$

Where G is the conductance (S), K is the electrode constant (K=9.76 cm⁻¹), σ is the conductivity (S/m), C_i is the concentrations (mol/m³), Z_i is the ion charge and λ_i is the molar ionic conductivities (Sm²/mol).

Fig. 8 shows the plots of conductance and pH, as a function of time. From Fig. 8A, the first part of the conductance plot shows a decrease in conductance, when

Table 3: Thermodynamic parameters for the adsorption of Zn(II) and Pb(II) on CaF₂.

	Temperature (K)	ΔG° (kJ/mol)	ΔS° (J/(molK))	ΔH° (kJ/mol)
Zn(II)	308	-7.2	23.3	5.5
	311	-7.3		
	328	-7.5		
	333	-7.7		
Pb(II)	308	-33.6	109.1	24.9
	311	-34.1		
	328	-35.2		
	333	-36.3		

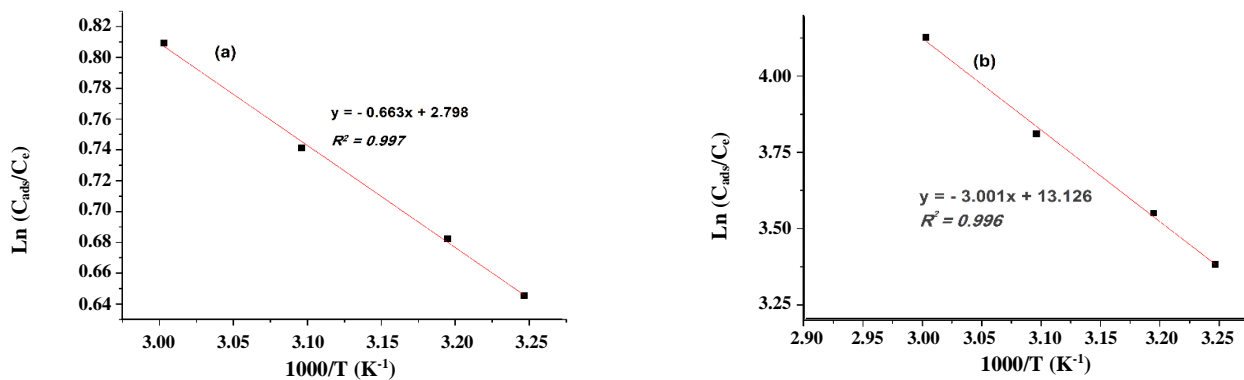


Fig. 7: Effect of temperature on the adsorption of (a) Zn(II) and (b) Pb(II).

Zn(II) and Pb(II) move to the solution. This result could be explained by the fact that the ionic mobilities ($\lambda(\text{Zn}^{2+})$ and $\lambda(\text{Pb}^{2+})$) are lower than $\lambda(\text{H}^+)$. From Fig. 8B, the first part of the pH plot indicates a shift to alkaline pH, which is in favor of the desorption of the Zn(II) and Pb(II) from CaF₂ to the solution. To maintain the electroneutrality in the solution, it could be considered that H⁺ are retained by CaF₂. The second part of the conductance and pH plots is characterized by a steadying of their evolution, which could be attributed to the existence of equilibrium between the adsorbed and desorbed ions. The total desorption is achieved after 120 s and 2000 s for Pb(II) and Zn(II), respectively. The result shows that the desorption yield reaches 89% for Zn(II) and 95% for Pb(II), which opens the route to regenerate the adsorbent for other cycles.

Competitive adsorption and desorption of Pb(II) and Zn(II)

Fig. 9a and Fig. 9b present respectively the conductance and conductivity as a function of time during

the competitive adsorption and desorption of Pb(II) and Zn(II). The results show the existence of two parts of straight line (Fig. 9a) probably due to a successive retention of the two metal ions. The solution analyses at 1500 s and 12000 s show that the adsorption capacities of Pb(II) and Zn(II) on CaF₂ are 93% and 78%, respectively. At 1500 s, the concentration of Zn(II) does not have an important change compared to Pb(II). This observation is in favor of the adsorption of Pb(II) for times lower than 1500 s. However, the adsorption of Zn(II) begins from 1500 s. Fig. 9b shows the presence of two parts; the first one could be attributed to the desorption of the two ions for $t < 900$ s due to the decrease of conductivity. This result is confirmed by the increase of pH until a value of 6 and its stabilization at a value of 7 (Figure S5, Supplementary information).

Fig. 10 shows the evolution of conductivity as a function of time (from 0 to 1200 s) during the competitive desorption of Pb(II) and Zn(II). Two segments of straight

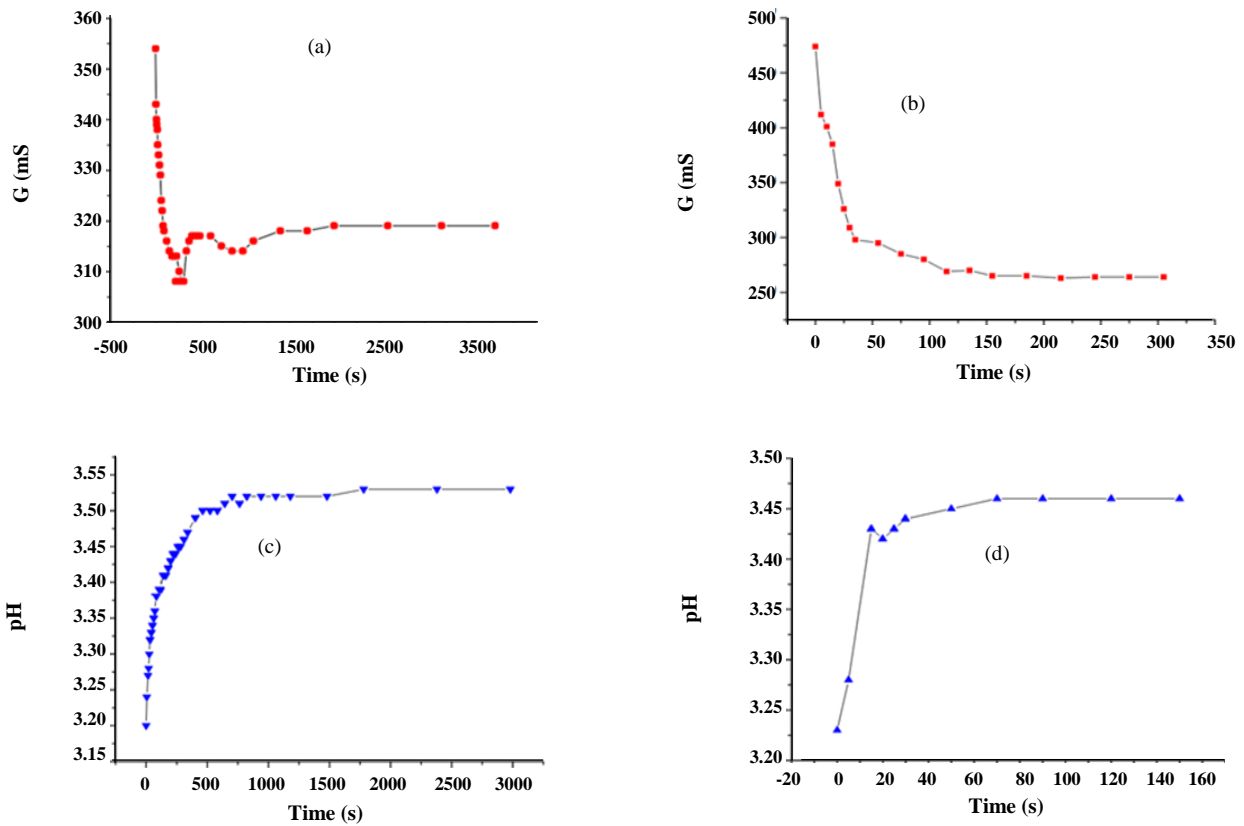


Fig. 8: (A) Conductance vs time: Desorption of (a) Zn(II), (b) Pb(II) and (B) pH vs time: Desorption of (c) Zn(II), (d) Pb(II).

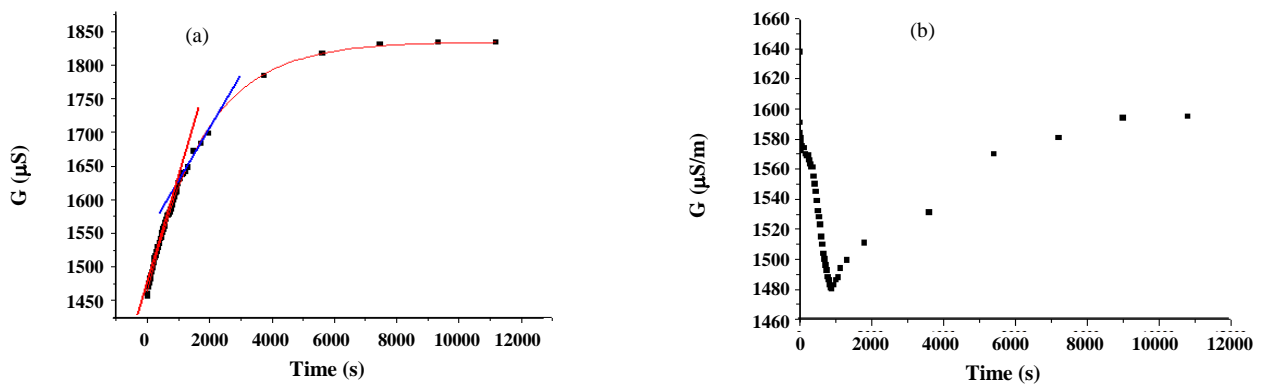


Fig. 9: (a) Conductance vs time for the competitive adsorption of Pb(II) and Zn(II), (b) Conductivity vs time for the competitive desorption of Pb(II) and Zn(II) [CaF_2 (1 g), $V=50$ mL of water, $\text{pH}=4$].

lines with different slopes at [0-420] and [421-900] could be observed, which is in favor of a consecutive desorption of the two ions. In fact, the solution analyses show that 89% of Zn(II) are desorbed below 420 s, and 95% of Pb(II) are desorbed at 900 s. Consequently, Zn(II) is desorbed before Pb(II) leading to a good separation selectivity.

CONCLUSIONS

CaF_2 nanoparticles were prepared by a facile one-step reaction and evaluated for the adsorption of Pb(II) and Zn(II) in aqueous solution. CaF_2 nanoparticles present high adsorption capacity and could be easily desorbed with HCl solution (0.01 M). The adsorption process fits well with the pseudo-second order kinetic model.

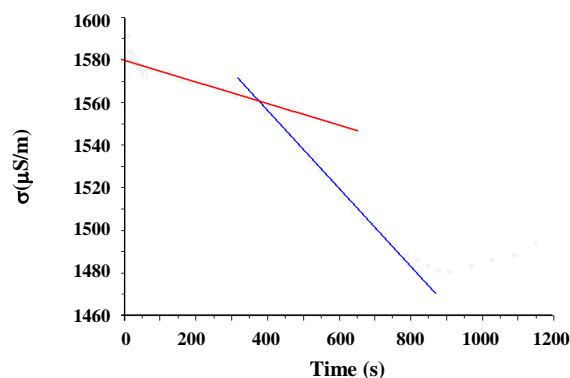


Fig. 10: Conductivity vs time for the competitive desorption of Zn(II) ([0-420]) and Pb(II) ([421-900]).

The adsorption of Zn(II) and Pb(II) is well described by Elovich and Langmuir isotherm models, respectively. The results show that Zn(II) is desorbed from CaF₂ before Pb(II) leading to a good separation. The desorption percentages reach 89% for Zn(II) and 95% for Pb(II). CaF₂ nanoparticles could be considered as an efficient adsorbent for the removal and separation of Zn(II) and Pb(II) from aqueous solution.

Acknowledgments

The authors gratefully acknowledge the financial support of the Ministry of Higher Education and Scientific Research of Tunisia.

Received : Mar. 29, 2019 ; Accepted : Jun. 10, 2019

REFERENCES

- [1] Ajam L., Ben Oueddou M., Sfar Felfoul H., El Mensi R., [Characterization of the Tunisian Phosphogypsum and Its Valorization in Clay Bricks](#), *Construction and Building Materials*, **23**: 3240-3247 (2009).
- [2] Tayibi H., Choura M., López F.A., Alguacil F.J., López-Delgado A., [Environmental Impact and Management of Phosphogypsum](#), *Journal of Environmental Management*, **90**: 2377-2386 (2009).
- [3] Mechi N., Khiari R., Ammar M., Elaloui E., Belgacem M.N., [Preparation and Application of Tunisian Phosphogypsum as Fillers in Papermaking Made from Prunus Amygdalus and Tamarisk sp.](#), *Powder Technology*, **312**: 287-293 (2017).
- [4] El-Didamony H., Ali M.M; Awwad N.S., Fawzy M.M., Attallah M.F., [Treatment of Phosphogypsum Waste Using Suitable Organic Extractants](#), *Journal of Radioanalytical and Nuclear Chemistry*, **291**: 907-914 (2012).
- [5] Tayibi H., Gasco C., Navarro N., Lopez-Delgado A., Choura M., Alguacil F.J., López F.A., [Radiochemical Characterization of Phosphogypsum for Engineering Use](#), *Journal of Environmental Protection*, **2**: 168-174 (2011).
- [6] Hentati O., Abrantes N., Caetano A.L., Bouguerra S., Gonçalves F., Römbke J., Pereira R., [Phosphogypsum as a Soil Fertilizer: Ecotoxicity of Amended Soil and Elutriates to Bacteria, Invertebrates, Algae and Plants](#), *Journal of Hazardous Materials*, **294**: 80-89 (2015).
- [7] Douahem H., Hammi H., Hamzaoui A., M'nif A., [Modeling and Optimization of Phosphogypsum Transformation into Calcium Fluoride Using Experimental Design Methodology](#), *Journal of the Tunisian Chemical Society*, **18**: 106-113 (2016).
- [8] Hajem B., Hamzaoui H., M'nif A., [Chemical Interaction Between Industrial Acid Effluents and the Hydrous Medium](#), *Desalination*, **206**: 154-162 (2007).
- [9] Hajem B., M'nif A., [Effect of Phosphogypsum Released Solution on Soil and Aquifer Water](#), *Asian Journal of Chemistry*, **23**: 4805-4809 (2011).
- [10] Gunathilake C., Kandanapitiye M.S., Dudarko O., Huang S.D., Jaroniec M., [Adsorption of Lead ions From Aqueous Phase on Mesoporous Silica with P-Containing Pendant Groups](#), *ACS Applied Materials & Interfaces*, **7**: 23144-23152 (2015).
- [11] Faghihian H., Rasekh M., [Removal of Chromate from Aqueous Solution by a Novel Clinoptilolite-Polyanillin Composite](#), *Iranian Journal of Chemistry and Chemical Engineering (IJCCE)*, **33**(1): 45-51 (2014).
- [12] Prasad M., Saxena S., Amritphale S.S., [Adsorption Models for Sorption of Lead and Zinc on Francolite Mineral](#), *Industrial & Engineering Chemistry Research*, **41**: 105-111 (2002).
- [13] Ruedas-Rama M.J., Hall E.A.H., [Azamacrocyclic Activated Quantum Dot for Zinc Ion Detection](#), *Analytical Chemistry*, **80**: 8260-8268 (2008).

- [14] Gul S., Waheed S., Ahmad A., Khan S.M., Hussain M., Jamil T., Zuber M., **Synthesis, Characterization and Permeation Performance of Cellulose Acetate/Polyethylene Glycol-600 Membranes Loaded with Silver Particles for Ultra Low-Pressure Reverse Osmosis**, *Journal of the Taiwan Institute of Chemical Engineers*, **57**: 129-138 (2015).
- [15] Rao G.P., Lu C., Su F., **Sorption of Divalent Metal Ions from Aqueous Solution by Carbon Nanotubes: A Review**, *Separation and Purification Technology*, **58**: 224-231 (2007).
- [16] Uddin M.K., **A Review on the Adsorption of Heavy Metals by Clay Minerals, with Special Focus on the Past Decade**, *Chemical Engineering Journal*, **308**: 438-462 (2017).
- [17] Sekar M., Sakthi V., Rengaraj S., **Kinetics and Equilibrium Adsorption Study of Lead(II) onto Activated Carbon Prepared from Coconut Shell**, *Journal of Colloid and Interface Science*, **279**: 307-313 (2004).
- [18] Akar T., Kaynak Z., Ulusoy S., Yuvaci D., Ozsari G., Akar S.T., **Enhanced Biosorption of Nickel(II) Ions by Silica-Gel-Immobilized Waste Biomass: Biosorption Characteristics in Batch and Dynamic Flow Mode**, *Journal of Hazardous Materials*, **163**: 1134-1141 (2009).
- [19] Ishaq M., Saeed, K., Imtiaz A., Sirraj S., Sohail A., **Coal Ash as a Low-Cost Adsorbent for the Removal of Xylenol Orange from Aqueous Solution**, *Iranian Journal of Chemistry and Chemical Engineering (IJCCE)*, **33**(1): 53-58 (2014).
- [20] Du Y.J., Hayashi S., **A Study on Sorption Properties of Cd²⁺ on Ariake Clay for Evaluating Its Potential Use as a Landfill Barrier Material**, *Applied Clay Science*, **32**: 14-24 (2006).
- [21] Gupta K., Bhattacharya S., Chattopadhyay D., Mukhopadhyay A., Biswas H., Dutta J., Ray N.R., Ghosh U.C., **Ceria Associated Manganese Oxide Nanoparticles: Synthesis, Characterization and Arsenic(V) Sorption Behavior**, *Chemical Engineering Journal*, **172**: 219-229 (2012).
- [22] Ahmadi S. H., Davar P., Manbohi A., **Adsorptive Removal of Reactive Orange 122 From Aqueous Solutions by Ionic Liquid Coated Fe₃O₄ Magnetic Nanoparticles as an Efficient Adsorbent**, *Iranian Journal of Chemistry and Chemical Engineering (IJCCE)*, **35**(1): 63-73 (2016).
- [23] Da'na E., **Ceria Associated Manganese Oxide Nanoparticles: Synthesis, Characterization and Arsenic(V) Sorption Behavior**, *Microporous and Mesoporous Materials*, **247**: 145-157 (2017).
- [24] Balistrieri L.S., Murray J.W., **The Surface Chemistry of Goethite (A-Feooh) in Major Ion Seawater**, *American Journal of Science*, **281**: 788-806 (1981).
- [25] Tahvildari K., Esmailipour M., Ghammamy S., Nabipour H., **Caf₂ Nanoparticles: Synthesis and Characterization**, *International Journal of Nano Dimension*, **22**: 269-273 (2012).
- [26] Marco-Lozar J.P., Juan-Juan J., Suárez-García F., Cazorla-Amorós D., Linares-Solano A., **MOF-5 and Activated Carbons as Adsorbents for Gas Storage**, *International Journal of Hydrogen Energy*, **37**: 2370-2381 (2012).
- [27] Giudici G.D., Biddau R., D'Incau M., Leoni M., Scardi P., **Dissolution of Nanocrystalline Fluorite Powders: An Investigation by XRD and Solution Chemistry**, *Geochimica et Cosmochimica Acta*, **69**: 4073-4083 (2005).
- [28] Ohashi Y., Nomura M., Tsunashima Y., Ando S., Sugitsue N., Ikeda Y., Tanaka Y., **Technique for Recovering Uranium from Sludge Like Uranium-Bearing Wastes Using Hydrochloric Acid**, *Journal of Nuclear Science and Technology*, **51**: 251-265 (2014).
- [29] Xiang W., Liu J., Chang M., Zheng C., **The Adsorption Mechanism of Elemental Mercury on CuO (110) Surface**, *Chemical Engineering Journal*, **200-202**: 91-96 (2012).
- [30] Langmuir I., **The Constitution and Fundamental Properties of Solids and Liquids Part I. Solids**, *Journal of the American Chemical Society*, **38**: 2221-2295 (1916).
- [31] Temkin, M.I., Pyzhhev, V., **Kinetics of Ammonia Synthesis on Promoted Iron Catalyst**, *Acta Phy. Chem*, URSS **12**: 327-356, (1940)
- [32] Dubinin M.M., **The Potential Theory of Adsorption of Gases and Vapors for Adsorbents With Energetically Nonuniform Surfaces**, *Chemical Reviews*, **60**: 235-266 (1960).
- [33] Dawodu F.A., Akpomie G.K., Ogbu I.C., **Isotherm Modeling on the Equilibrium Sorption of Cadmium(II) from Solution by Agbani Clay**, *International Journal of Multidisciplinary Sciences And Engineering*, **3**: 9-14 (2012).

- [34] Mohamad Ibrahim M.N., Wan Ngah W.S., Norliyan M.S., Wan Daud W.R., Rafatullah M., Sulaiman O., Hashim R., [A Novel Agricultural Waste Adsorbent for the Removal of Lead\(II\) Ions from Aqueous Solutions](#), *Journal of Hazardous Materials*, **182**: 377-385 (2010).